MODELING THE GRAMICIDIN CHANNEL

Interpretation of Experimental Data Using Rate Theory

G. EISENMAN
Department of Physiology, University of California Los Angeles Medical School, Los Angeles, California 90024

J. P. SANDBLOM
Department of Physiology and Medical Biophysics, University of Uppsala, Uppsala, Sweden

A three-barrier two-site Eyring model (4) has become accepted for the gramicidin channel (6), but more extensive measurements (1) indicate certain inadequacies (12, 1). Although these could conceivably represent inherent limitations of the Eyring approach (7, 8), we have extended (3) the above model by adding a site external to the barrier at the channel mouth at each end of the channel and in equilibrium with the adjacent solution. In contrast to other models (5) that reduce the number of free parameters by making specializing assumptions as to the kinds of interactions that could be occurring (e.g., solely electrostatic), no such restrictions were introduced before data-fitting; the behavior of the parameters themselves can be interpreted in terms of the kinds of interactions actually taking place. We examine this model here to demonstrate its phenomenological adequacy for Li, Na, K, Rb and Cs, and to discuss some of the physical implications of the calculated parameters, particularly as to binding and permeation. (For a discussion of ionic interactions with each other and with the channel, see reference 2.) We should point out that the existence of the additional site can be rationalized not only on theoretical grounds (reference 3, Fig. 1) and as a necessary bookkeeping device (reference 10, footnote 10) but also, independently, from the blocking effects of the impermeant tetraethylammonium ion (15).

Fig. 1 plots the experimentally observed (1, 2) *I-V* shape for Li, Na, K, Rb and Cs as three-dimensional plots of I/G° vs. voltage and vs. log ionic activity. At the lower right are also plotted the single channel conductances (G°) at different permeant ion activities. The curves are theoretical. Clearly the extended model adequately describes the electrical data in glyceryl monooleate (GMO) bilayers. It also is satisfactory (2) for the flux ratio exponents in diphytanoyl phosphatidylcholine (DPPC) (13).

Besides the satisfactory agreement between experiment and theory, the following should be particularly noted. First, significant changes in *I-V* shape occur at concentrations below those used in previous comparisons (4, 9) for which the lowest concentration was 5–10 mM. Such changes are particularly important in the case of Cs, for which the shape in the low concentration limit is crucial to arguments for interfacial polarization (10). Fig. 1 shows that a measurement of the true low-concentration limiting shape must be performed at concentrations 10–100 times lower than the 10 mM used (10), for only in the true low-concentration limit does the *I-V* shape reflect only the voltage dependence of the entry step. Thus, the linear dependence of *I* upon *V* at high voltage observed at 10 mM (10), interpreted as resulting from interfacial polarization, is also seen in the *I-V* data in Fig. 1; but this linear dependence almost totally disappears at sufficiently low concentrations. This indicates that the *V*-dependence observed at 10 mM is still due to the exit step rather than the entrance step.

A second point to be noted is that important species differences exist in the *I-V* shapes in the limit of low ion concentration. These reflect differences in the energy profiles to be discussed below. Recall that the *I-V* shape in the limit of low ion concentration depends only upon the ratios of rate constants for crossing vs. leaving the channel, together with the voltage dependence of the entry step [12, 3].

In contrast to the agreement between the experimental data and the theoretical expectations of the four-site model (Fig. 1), we have not been able to obtain a satisfactory fit with the 3B2S model, even when extending it by allowing the positions of the energy wells and barriers to shift with differing occupancy.

The physical implications of the model parameters will now be discussed. Fig. 2 plots the energy profile (in the potential field) for one-ion occupancy by the indicated cations calculated from the rate constants and binding constants corresponding to the theoretical curves of Fig. 1. The figure makes it apparent that there are clear species differences in the positions and magnitudes of the barriers and wells.

Consider first the locations of the barriers and wells for the group I*a* cations. Whereas the top of the entrance barrier lies almost at the mouth of the channel for the larger ions, it moves increasingly inwards as the ions become smaller. A parallel behavior is seen for the location of the inner binding site, which lies increasingly deeper as the ions become smaller. In consequence, the voltage dependence for leaving the channel is much larger for the smaller ions than for the larger ones.

From examining the levels of the peaks it is clear that

BIOPHYS. J. © Biophysical Society · 0006-3495/84/01/88/03 $1.00
Volume 45 January 1984 88–90

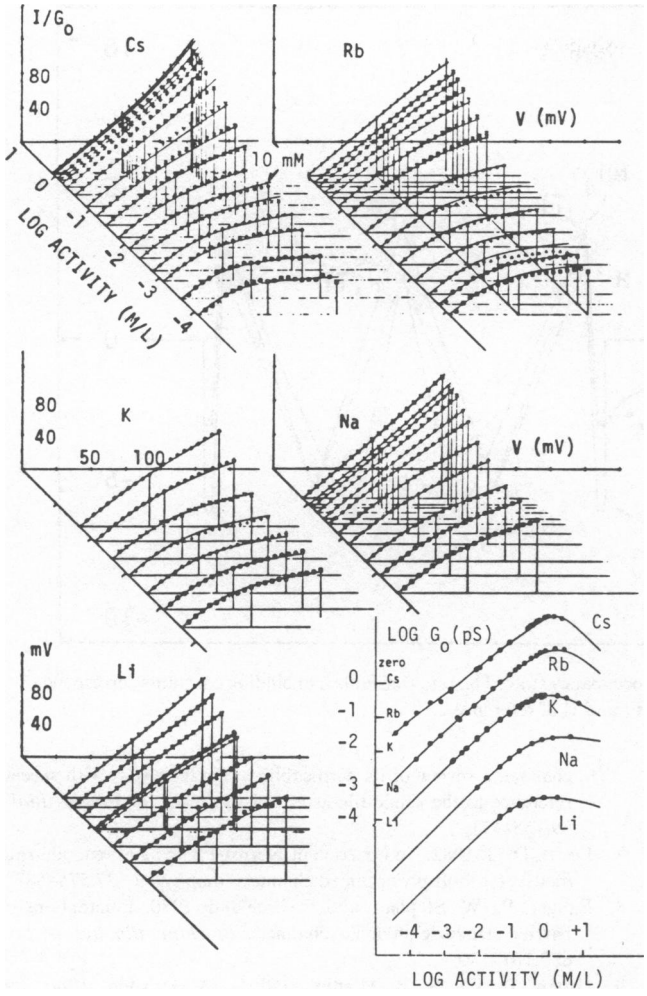

FIGURE 1 Comparison of experimental data with theoretical expectations for the *I-V* shape (plotted as I/G^o) and zero current conductance (G^o) for the five group I*a* cations. Described in text. All measurements were made on GMO bilayers; the many-channel *I-V* data were corrected for capacitative currents by subtracting the currents recorded from bare bilayers at comparable salt concentrations, frequencies and voltages (see references 1, 2, 11 for details). A nonlinear least-squares (Levenberg-Marquardt) algorithm developed by Chris Clausen for simultaneously fitting multiple data sets and several theoretical functions was used to obtain the model parameters. Published values for single channel conductances at low voltage (50 mV) (11) have been supplemented by noise measurements at ultra-low concentrations (Neher, Eisenman, and Sandblom, unpublished). The values of G^o were calculated from data measured at 50 mV using the I/G^o shapes at the appropriate concentrations to extrapolate back to zero applied potential. The points are experimental; their reproducibility from experiment to experiment is generally better than the size of the symbols. The *I-V* curve in Cs at 10 mM, discussed extensively in the text, is labeled.

the permeability to larger ions is greater than that to smaller ions (i.e., the peak energies for the larger ions are less elevated above the aqueous reference level than are those of the smaller ions). Despite this, the larger ions have more difficulty entering, crossing, and leaving the channel than do the smaller ions because they see larger barriers for entry, crossing, and exit. For example, the difference in entrance barrier heights (the height of the entrance peak above the outer site) for Li vs. Cs corresponds to an entrance rate constant of 1.9×10^8 s^{-1} for Li vs. 4.6×10^5 s^{-1} for Cs (2). This exemplifies how a high binding affinity can offset a low jumping rate to give a high permeability.

Note that, contrary to the low selectivity observed for the overall permeation process, as judged by reversal potential or conductance at the usual concentrations (9), there is substantial binding selectivity, as well as rate selectivity, apparent in the large differences in the depths of the wells and heights of the barriers in Fig. 2. For example, the affinity of the outer site differs by a factor of 7,000 between Cs and Li, while that for the inner site differs by a factor of 400 (reference 2, Table I).

The profiles for H, NH_4 and Tl indicate that these species differ only quantitatively from the other monovalent cations. In particular, the locations of the sites and barriers are rather similar in the case of Tl and NH_4 to those for group I*a* cations of comparable size (K and Rb). Energetically, the profile for Tl also seems reasonable for a polarizable species of its size since the deeper wells indicate a stronger binding than for K and Rb. The rate constants for entry and exit are correspondingly slower, but the rate constant for crossing lies between that for Rb and K, as would be expected from size alone.

The profile for H is of interest in its striking similarity to that for NH_4. For both species, the sites and barriers are located at the same places; but the barriers for entering, leaving and crossing are all smaller by ~1.4 KCal/M for H than for NH_4, consistent with the rate constants being ~10 times faster for H than for NH_4. This result suggests that the binding of both H (actually H_3O) and NH_4 involves H-bonds to channel ligands, and that a Grotthuss jump process is available for H consistent with its ability to slip past any water "plug" (16).

Besides the above differences in energy profile for the one-ion–occupied channel, systematic effects of occupancy on the energy profile are also implied by the finding that the rate constants and binding constants vary systematically with occupancy as well as with ion size, as discussed elsewhere (2).

Finally, certain assumptions made in developing the theory should be noted. A rate theory approach may be thought of as a limiting case of a continuum formulation (7) where the energy barrier is so steep that the kinetics become dominated by the energy at the peak. The fundamental limitations of rate theory have to do with its description of nonequilibrium phenomena using equilibrium properties of the system, an approach valid only where the time needed for the adjustment of ligands after an ion jump is small compared to the dwelling time in the potential well (8). We have assumed, for simplicity, that the energy profile is instantly established for a given occupancy state. If this should not be strictly correct, the physical interpretation should still apply to a time-averaged state of the system. We have also assumed that

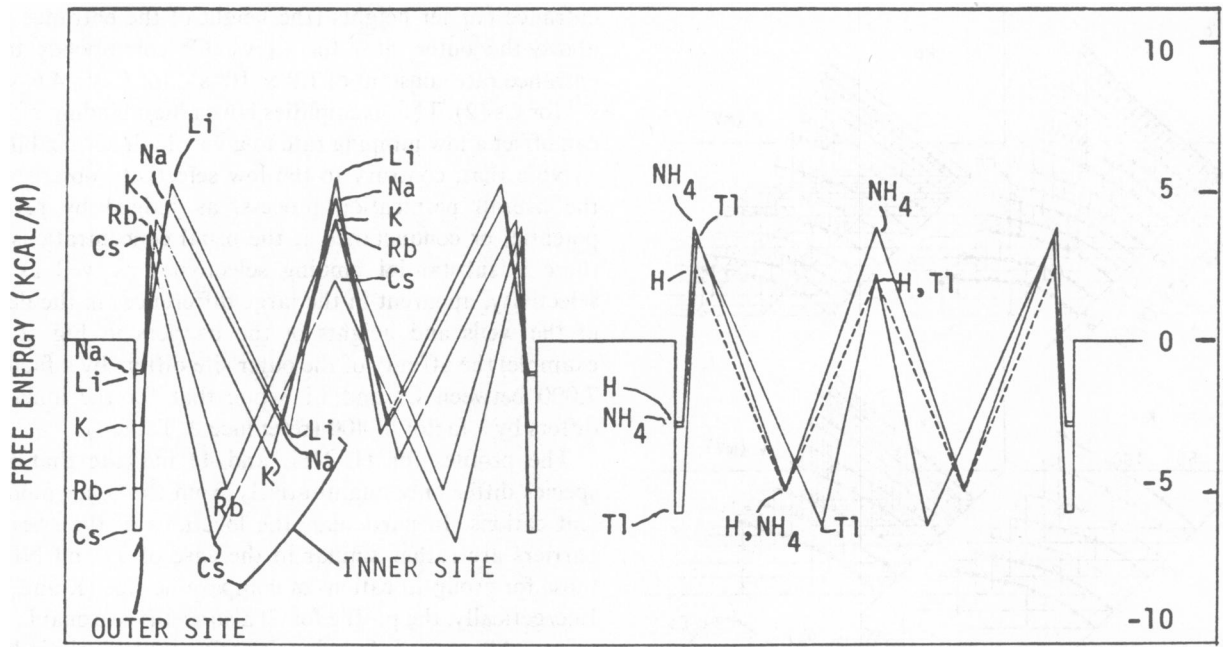

FIGURE 2 Free energy profiles for the indicated cations in the one-ion–occupancy state. The rate constants and binding constants correspond to those required to fit the data of Fig. 1; their values are given in Tables I and II of reference 2.

the outer site lies external to any applied potential field and that the locations of sites and barriers, while allowed to differ among the species, remain invariant for different loading states. These assumptions can be relaxed should this become warranted.

This work was supported by grant PCM 76-20605 from the National Science Foundation and grant GM 24749 from the U. S. Public Health Service.

Received for publication 6 May 1983.

REFERENCES

1. Eisenman, G., J. Sandblom, and J. Hägglund. 1983. Electrical behavior of single-filing channels. *In* Structure and function in excitable cells. W. Adelman, W. Chang, R. Leuchtag and I. Tasaki, editors. Plenum Publishing Corp., New York. 383–411.
2. Eisenman, G., and J. Sandblom. 1983. Energy barriers in ionic channels: data for gramicidin A interpreted using a single-file (3B4S") model having 3 barriers separating 4 sites. *In* Physical Chemistry of Transmembrane ion motions. G. Spach, editor. Elsevier/North Holland Biomedical Press, Amsterdam. 329–348.
3. Sandblom, J., G. Eisenman, and J. V. Hägglund. 1983. Multi-occupancy models for single-filing ionic channels. Theoretical behavior of a 4-site channel with 3 barriers separating the sites. *J. Membr. Biol.* 71:61–78.
4. Urban, B. W., and S. B. Hladky. 1979. Ion transport in the simplest single-file pore. *Biochim. Biophys. Acta.* 554:410–429.
5. Urry, D. W., C. M. Venkatachalam, A. Spisni, R. J. Bradley, T. L. Trapane, and K. U. Prasad. 1980. The malonyl gramicidin channel: NMR-derived rate constants and comparison of calculated and experimental single-channel current. *J. Membr. Biol.* 55:29–51.
6. Finkelstein, A., and O. S. Andersen. 1981. The gramicidin A channel: a review of its permeability characteristics with special reference to the single-file aspect of transport. *J. Membr. Biol.* 59:155–171.
7. Levitt, D. G. 1982. Comparison of Nernst-Planck and reaction-rate models for multiply occupied channels. *Biophys. J.* 37:575–587.
8. Läuger, P., W. Stephan, and E. Frehland. 1980. Fluctuations of barrier structure in ionic channels. *Biochim. Biophys. Acta.* 602:167–180.
9. Urban, B. W., S. B. Hladky, and D. A. Haydon. 1980. Ion movements in gramicidin pores. An example of single-file transport. *Biochim. Biophys. Acta.* 602:331–354.
10. Andersen, O. S. 1983. Ion movement through gramicidin A channels. Interfacial polarization effects on single-channel current measurements. *Biophys. J.* 41:147–165.
11. Neher, E., J. Sandblom, and G. Eisenman. 1978. Ionic selectivity, saturation, and block in gramicidin A channels. II. Saturation behavior of single-channel conductances and evidence for the existence of multiple binding sites in the channel. *J. Membr. Biol.* 40:97–116.
12. Eisenman, G., J. Hägglund, J. Sandblom, and B. Enos. 1980. The current-voltage behavior of ion channels: important features of the energy profile of the gramicidin channel induced from the conductance-voltage characteristic in the limit of low ion concentrations. *Upsala J. Med. Sci.* 85:247–257.
13. Procopio, J., and O. S. Andersen. 1979. Ion tracer fluxes through gramicidin A modified lipid bilayers. *Biophys. J.* 25(2,Pt.2):8 *a.* (Abstr.)
14. Bamberg, E., and P. Läuger. 1977. Blocking of the gramicidin A channel by divalent cations. *J. Membr. Biol.* 35:351–375.
15. Eisenman, G., and J. Sandblom. 1983. TEA and TMA alter the *I-V* characteristics of the gramicidin channel as if they bind to channel sites at differing depths in the potential field but do not cross. *In* The Physiology of Excitable Cells. A. Grinnell and W. Moody, editors. Alan R. Liss, New York. pp. 191–204.
16. Levitt, D. G., S. R. Elias, and J. M. Hautman. 1978. Number of water molecules coupled to the transport of sodium, potassium and hydrogen ions via gramicidin, nonactin or valinomycin. *Biochim. Biophys. Acta.* 512:436–451.